Generation of elastic waves from line and point sources by a high-current pulse method

Kwang Yul Kim and Wolfgang Sachse

Citation: The Journal of the Acoustical Society of America **86**, 875 (1989); doi: 10.1121/1.398721
View online: https://doi.org/10.1121/1.398721
View Table of Contents: https://asa.scitation.org/toc/jas/86/3
Published by the Acoustical Society of America

Generation of elastic waves from line and point sources by a high-current pulse method

Kwang Yul Kim and Wolfgang Sachse
Department of Theoretical and Applied Mechanics, Cornell University, Ithaca, New York 14853

(Received 23 August 1988; accepted for publication 12 May 1989)

This paper describes a method of generating both line and point sources of acoustic emission (AE) signals by a powerful, transient Joule heating of a thin, conductive film deposited on an insulating plate or a small diameter metal wire buried inside it. Point-and line-source AE signals are generated by heating a short or a long section of thin film, respectively. The versatility of this method is demonstated by the diversity of AE signals that can be produced by simply changing the rise time, magnitude, and duration of the current pulse that provides the heating. An analysis shows that both the line and the point AE sources are of dipolar type for the case of the heated thin film. The line source resulting from an imbedded long, thin wire appears to be a two-dimensional center of dilatation. Short-duration current pulses generate a step source whose rise time is approximately equal to that of the input electrical power pulse while long-current pulses produce a linear ramp source that resembles the temperature rise of the heated conducting film or wire.

PACS numbers: 43.88.Ar, 43.40.Le, 43.35.Ud

INTRODUCTION

The generation of acoustic or elastic waves accompanying the transient, short-duration thermal heating of a material is rapidly becoming a powerful tool for the characterization of materials and the imaging of their microstructures. Point-source ultrasonic signals can be produced by using Q-switched laser beams to strike a small spot on a specimen's surface. Several reviews have appeared summarizing the work with laser-generated ultrasound.[1-3] Detection of the acoustic signals near a specimen placed in an intensity-modulated laser beam forms the basis of the photo-acoustic spectroscopy (PAS) technique.[4] Similarly, the use of a pulsed or modulated continuous wave laser beam in a scanning mode over a specimen surface has been adapted to image material microstructures.[5,6] Other thermal sources have also been used to generate acoustic signals. Reported has been the use of pulsed or modulated beams of electrons in an electron microscope[7] and ions[8] with detection of the signals by a piezoelectric transducer or an optical beam deflection technique (c.f. Refs. 9 and 10). Kim and Sachse[11,12] have used an intense, pulsed x-ray beam for the generation of thermoelastic waves and discussed its potential application to materials characterization problems.

It is then quite natural to expect that thermoelastic waves can also be generated by a transient electrical Joule heating of a localized zone in a material. Localized heating can be achieved with the deposition of a thin metal film of narrow width on an insulating plate such as glass, a semiconductor, or a ceramic material, or with burying a thin metallic wire inside an insulator and finally by sending a high-current pulse of various durations and magnitudes through it. Although the principal motivation of this research was to investigate the adhesive and thermal characteristics of thin films deposited on a substrate, in this paper we are dealing with the generation of thermoelastic waves and a determination of their source characteristics. The results of our investigation on the adhesion of thin metal films on a substrate will be presented in another paper.[13]

The advantage of using an electrical power to generate elastic waves in solids lies in its simplicity and versatility in generating waves of various shapes and amplitudes through control of the electrical excitation rise time, duration, and magnitude, and its relatively low cost in comparison with the other methods mentioned above. It is also expected that a variety of thermoelastic waves of different sources can be generated by using ingenious patterns of thin films deposited on a substrate. Such patterns are readily realizable by modern semiconductor fabrication techniques.

In the following section we describe the experimental setup used to make the measurements. The objective of Sec. II is to formulate the theory of a dipole source of acoustic emission and the thermoelastic waves it generates. In Sec. III experimental data are presented, analyzed, and compared with the theory by using the results of Sec. II and a signal deconvolution technique. The source-time functions of the dipolar sources are discussed in Sec. IV in terms of the mismatch of thermal expansions between the thin film and the substrate. In the final section are some concluding remarks.

I. EXPERIMENT

Essential for the generation of detectable thermoelastic waves is a powerful current pulse generator that can deliver a pulse strong enough to cause a temperature rise of an order of a few tens of degrees (in °C) over a time interval ranging from submicroseconds to several tens of microseconds. A high, nearly constant current pulse generator that can deliver a maximum power of 20 kW for a time interval up to 0.5 ms with a repetition rate of 10 pulses/s was especially designed and fabricated in our laboratory for this. The condition of constant current for a long-duration pulse, whose

 0001-4966/89/090875-10$00.80

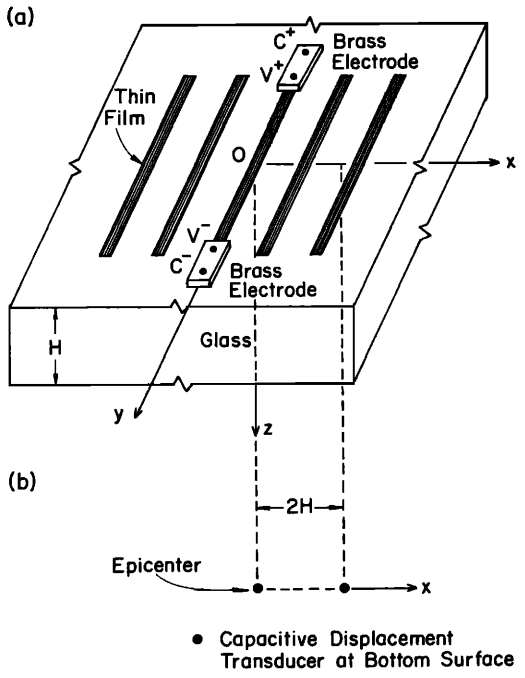

FIG. 1. (a) Schematic of the thin-film layout on the substrate for generation of elastic waves. (b) Location of the capacitive transducers.

duration is longer than 10 μs, is desirable because it facilitates a theoretical analysis of the temperature behavior of the heated zone. It is not, however, an essential requirement for generating thermoelastic waves or for investigating their source characteristics.

The insulating material chosen as the substrate for the thin-film deposition was a glass plate, 15 cm long, 15 cm wide, and 0.968 cm thick. As shown in Fig. 1, several identical, parallel, thin-film strips, about 10 cm long and 0.5 cm apart from each other, were deposited on the top side of the plate. While it is possible to use medium conductivity materials such as titanium, nickel, or chromium for the thin films, the materials used for deposition were chosen for their high electrical conductivity which minimizes the total resistance of the film and thus permits delivery of maximum power to it. One of the films was silver, 2 mm wide and 0.5 μm thick, deposited on a glass plate by sputtering. The other was aluminum, 1.5 mm wide and 1 μm thick, evaporated onto the plate. The entire bottom side of each plate was coated with a 0.3-μm-thick chromium film to serve as a ground plane for the capacitive displacement transducers used to detect the normal surface motions caused by the thermoelastic waves propagating through the plate.[14] Two capacitive transducers were used with one located at epicenter and the other located at $2H$ away from epicenter. Here, H is the plate thickness. The diameter of the circular electrode of the capacitive transducer used was 3 mm. The specimen surface facing the capacitor electrode is essentially traction-free and no diffraction of elastic waves was observed in the detected signals due to the presence of the capacitive transducers. Two small polished brass plates were attached on top of the same thin-film strip by using a silver epoxy cement. The spacing between them (or the two brass plates) on the silver thin film was 2 mm for the point source and about 10 cm for the line source obtained with the thin film of aluminum. Each brass plate has two electrodes with one used for the excitation current and the other for the potential measurement.

The block diagram of the entire electronic measurement system is shown in Fig. 2. A high-current pulse with magnitude ranging from several to 100 A and with duration ranging from a few to 100 μs was fed from the generator to the thin film. The magnitude of the current flowing through the film was measured by an ac current probe that had a bandwidth from 120 Hz to 60 MHz. The output of the current probe and the voltage across the thin film were both digitized in a two-channel waveform recorder that was operating at a 30-MHz sampling rate with 10-bit resolution. The output of the capacitive transducers was amplified by charge amplifiers whose bandwidth extended from 10 kHz to 10 MHz and their output was digitized by a second digitizer operating at the same sampling rate as the first. Both digitizers were operating in the post-trigger mode in synchronization with an external trigger pulse derived from the current pulse generator. In this mode, the detected signals are recorded after the arrival of the trigger signal. The recorded waveforms in the digitizers were displayed on an x-y scope and were transferred to an interactive microcomputer-based data acquisition system for data storage and their analysis.

It was observed that the initial portion of the capacitive sensor signals lasting less than 2 μs around the first P-(longitudinal) wave arrival were corrupted with an electromagnetic pickup apparently caused by the mutual inductance between the capacitor elements and the thin-film circuit when the excitation current was suddenly applied. This problem was circumvented by reversing the current flow through the film, which gave rise to an electromagnetic noise signal of equal magnitude but of opposite sign. These two signals, corresponding to the forward and reverse currents, were subsequently added in order to eliminate almost entirely the electromagnetic noise from the detected signals and it

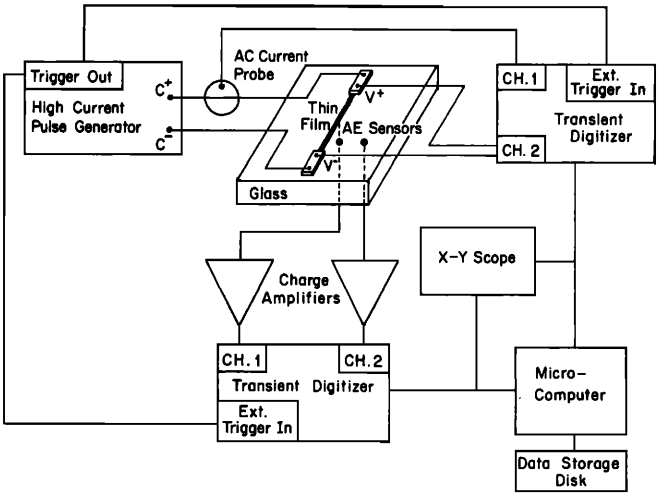

FIG. 2. Electronic block diagram of line- and point-source AE generation and their detection system.

is this resulting signal which is shown in all the results to follow.

II. THEORY

A thin metal film, heated by the resistance to the flow of an electrical current, will expand freely in the absence of a substrate. However, when the film is attached to a substrate, the thermal expansion of the film is constrained by the film/substrate interface. If the linear coefficients of thermal expansion of the metal film and a glass substrate are denoted by α_f and α_s, respectively, then the force exerted by the film on the glass at the interface per unit length of the film is given by

$$f = [cdE_f/(1-\nu_f)](\alpha_f - \alpha_s)\theta_f, \tag{1}$$

where θ_f, E_f, ν, and w are the temperature rise, Young's modulus, Poisson's ratio, and the thickness of the film, respectively, and c is a dimensionless constant very close to unity. This outward force acts in a direction perpendicular to the film strip as indicated in Fig. 3, thus constituting a horizontal dipole force. The horizontal dipole force acted as an acoustic emission (AE) source which excited various wave modes, including longitudinal, shear, and Rayleigh waves. If an AE sensor is located on the thin-film side of the specimen plate, the Rayleigh wave arrival is expected to be a dominant mode in the detected signal. The thickness of the thin film d should be thin enough (such that $d \ll \sqrt{k_f t}$, where k_f is the thermal diffusivity of the film material) to ensure the uniform temperature through the thickness in the time interval of interest, resulting in an excitation of the horizontal dipole source only. A conservative estimate for most metals is that $d \leqslant 10\,\mu$m.

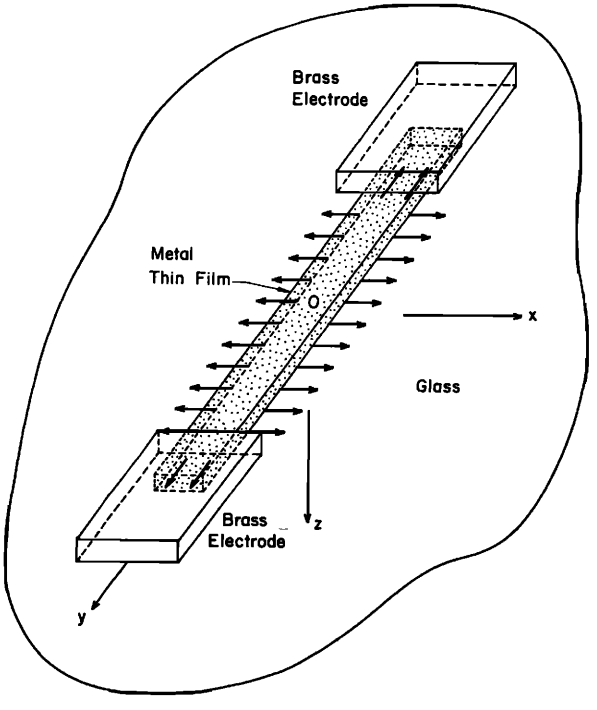

FIG. 3. Diagram showing a dipole force generated as a result of abrupt heating of the thin film.

The temperature rise in the film, given by θ_f, for the case of a long strip operating as a line source, can be computed theoretically from a solution of heat balance equation in which the effects of the brass electrodes at both ends of the film are neglected and by assuming that the temperature is uniform throughout the film. The latter is probably well justified since the film is less than 1 μm thick. If A, C_P, and R, respectively, denote the total area, bulk specific heat, and electrical resistance of the thin film between the two brass electrodes, then the balance of heat energy requires that

$$I^2R = C_P \frac{\partial \theta_f}{\partial t} + A(h\theta_f + k_s[\nabla\theta_s]_{z=0}), \tag{2}$$

where t represents time, h is the surface heat conductance, k_s is the thermal conductivity of the glass substrate, $[\nabla\theta_s]_{z=0}$ is the temperature gradient at the film/substrate interface, and I is the current flowing through the film. Here, θ_s denotes a temperature rise in the substrate.

In this paper we are only interested in the solution of Eqs. (1) and (2) over a time interval corresponding to the duration of the heating pulse. In our case this was less than 100 μs, for which the thermal diffusion distance $\sqrt{\kappa_s t}$ in glass is 7.5 μm, where $\kappa_s = 0.0056\ \text{cm}^2/\text{s}$ is the thermal diffusivity of glass. If the origin of the coordinate system is taken to be at the surface of the film and the z-coordinate axis points into the substrate while the x-coordinate axis is perpendicular to the film strip as shown in Fig. 3, then the term $[\nabla\theta_s]_{z=0}$ in Eq. (2) can be replaced by $\partial\theta_s/\partial z$ at $z=0$, since $\sqrt{\kappa_s t}$ is much smaller than w, the width of the film. Writing the resistance of the film R in the form

$$R = R_0(1+\gamma\theta_f), \tag{3}$$

where R_0 is the initial resistance of the film and γ is the temperature coefficient of unit resistance, one obtains, from Eq. (2),

$$I^2R_0(1+\gamma\theta_f) = C_P\frac{\partial\theta_f}{\partial t} + A\left(h\theta_f + k_s\frac{\partial\theta_s}{\partial z}\bigg|_{z=0}\right). \tag{4}$$

Since there is no heat source or sink in the substrate,

$$\frac{\partial^2\theta_s}{\partial z^2} = \kappa_s\frac{\partial\theta_s}{\partial t} \tag{5}$$

holds in glass with initial conditions $\theta_f = \theta_s = 0$ at $t=0$. Equations (4) and (5) are coupled and the increase in the temperature of the film is obtained from their solution at $z=0$. The solution can be conveniently found by employing a Laplace transform technique as discussed in Chap. 12 in the text of Carslaw and Jaeger.[15]

When the current I remains constant during the duration of the current pulse, an analytical solution can be easily obtained from which the bulk specific heat of the film[16,17] can be found:

$$C_P = I^2R_0\gamma/R_0'(0), \tag{6}$$

where $R_0'(0)$ denotes dR/dt at the initial time at $t=0$. When I is a slowly varying function of time, it can be expressed in polynomial form and the solution to Eqs. (4) and (5) can again be found using the Laplace transform technique. For a short-duration current pulse, whose analytical

form is difficult to express, an alternative is a numerical technique by which the solution can be obtained. The actual temperature rise in the thin film is easily obtained from the experimentally measured resistance data $R(t)$ and using Eq. (3). Since the analytical solution for $R(t)$ is not required for study of the generated elastic waves, it is not pursued further in this paper, although it is recognized to be an important element in investigations of the thermal properties of a thin film and a substrate.

A horizontal dipole associated with a point source having a short section of the film length Δl, located at y, should scale with the force f of Eq. (31) and the film width w. This can be written as

$$D_{xx}(y,t)\Delta l = f w\,\Delta l = c[E_f/(1-\nu_f)]wd\,\Delta l(\alpha_f-\alpha_s)\theta_f(t). \quad (7)$$

We note that a horizontal dipole function per unit length of the film in the x direction, $D_{xx}(y,t)$, is independent of y because of the homogeneity of the film and its uniform width and thickness along its length. A normal displacement $u_z^P(\mathbf{r},t)$ at location $\mathbf{r}$ and at time t resulting from a point dipole $D_{xx}(t)\Delta l$ can be expressed by means of the Green's function according to[18,19]

$$u_z^P(\mathbf{r},t) = \int_0^t D_{xx}(y,t)\Delta l\, G_{xz,x}^P(\mathbf{r},y;\,t-\tau)d\tau = D_{xx}(t)\Delta l * G_{xz,x}^P(\mathbf{r},y;\,t), \quad (8)$$

where G^P represents the Green's tensor associated with a point source and $*$ denotes a convolution integral in time. The displacement $u_z^l(\mathbf{r},t)$ resulting from a line source of length l is given by

$$u_z^l(\mathbf{r},t) = \int_0^l D_{xx}(t)*G_{xz,x}^P(\mathbf{r},y;\,t)dy = D_{xx}(t)*\int_0^l G_{xz,x}^P(\mathbf{r},y;\,t)dy = D_{xx}(t)*G_{xz,x}^l(\mathbf{r},t), \quad (9)$$

where

$$G_{xz,x}^l(\mathbf{r},t) \equiv \int_0^l G_{xz,x}^P(\mathbf{r},y;\,t)dy. \quad (10)$$

When l is sufficiently long, $G_{xz,x}^l(\mathbf{r},t)$ can be approximated by $G_{xz,x}^\infty(\mathbf{r},t)$, which is the Green's function corresponding to an infinitely long line source. If the time of interest is limited up to the arrival time τ_P^l, corresponding to the first P-(longitudinal) ray emanating from the ends of the line source, then,

$$G_{xz,x}^l(\mathbf{r},t) = G_{xz,x}^\infty(\mathbf{r},t), \quad \text{for} \quad 0 \leqslant t \leqslant \tau_P^l. \quad (11)$$

To maximize τ_P^l in Eq. (11), the acoustic sensors should be located at points midway between the ends of the long line segment of the film. In our experiments, this corresponded to a value of τ_P^l of approximately 9 μs.

Algorithms for computing the Green's function of the plate, which appear in Eq. (8), have been developed for the nearfield of a source by Ceranoglu and Pao[20] using a generalized ray theory. To compute the values of $G_{xz,x}^l$ we made use of Eq. (10), even though using Eq. (11) would be more convenient for times less than τ_P^l if $G_{xz,x}^\infty$ were available.

The Green's function for an epicentral receiver corresponding to a dipolar point source is shown in Fig. 4(a), while the Green's functions corresponding to a line source and receivers on the opposite side of the plate at the epicentral and $2H$ receiver positions are shown in Fig. 4(b) and (c), respectively. They are the displacement responses at the receiver point due to an impulse (δ-function) excitation. The longitudinal (P) and shear (S) wave speeds of glass used for calculating the above results were 0.582 and 0.350 cm/μs, respectively. The first longitudinal and shear wave arrivals are marked with P and S, respectively, in the figure. Finally, the dipole source-time functions, $D_{xx}(t)$ appearing in Eqs. (8) and (9) were calculated using a deconvolution technique both for point and line sources and for short- and long-duration excitation current pulses.

III. EXPERIMENTAL DATA AND RESULTS

A. Short pulse response

Shown in Fig. 5(a) and (b) are the measured excitation current pulse and the computed electrical power pulse equal

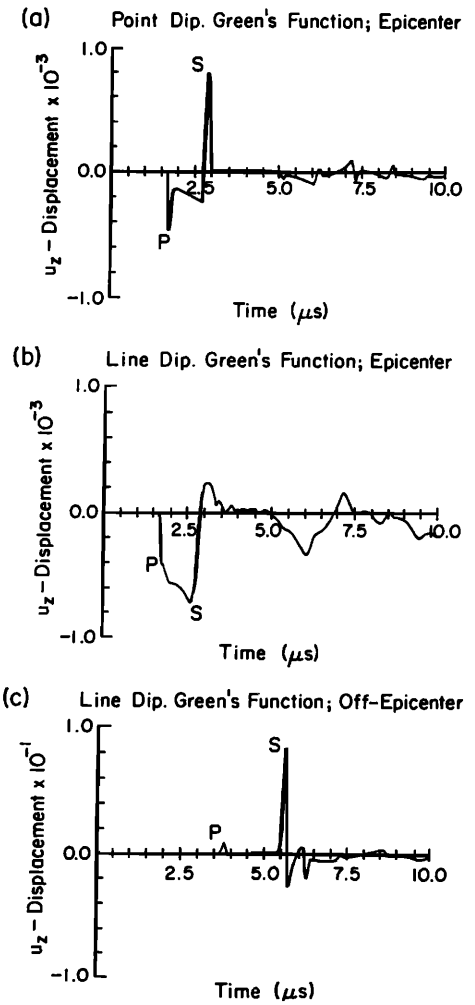

FIG. 4. Plate Green's functions. (a) Horizontal point dipole source, receiver at epicenter. (b) Horizontal line dipole source, receiver at epicenter. (c) Horizontal line dipole source, receiver at $2H$ away from epicenter.

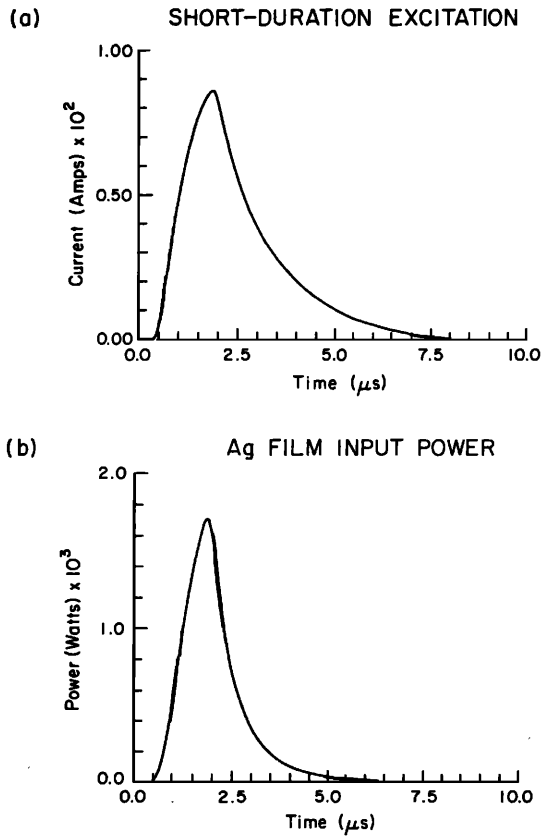

FIG. 5. (a) Excitation current pulse of short duration applied to a short section of silver film. (b) Excitation power pulse of short duration.

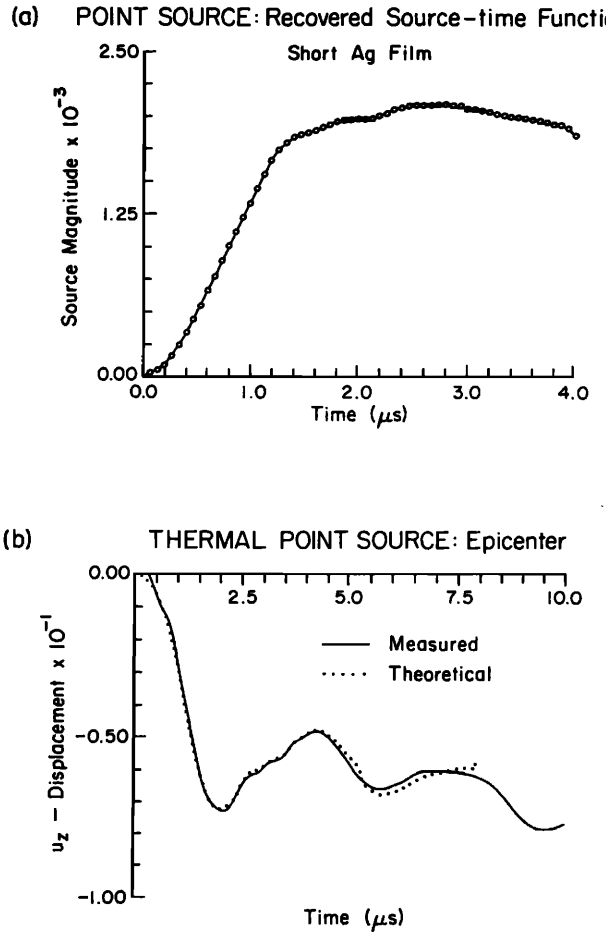

FIG. 6. (a) Point source dipole time function associated with the short-current pulse. (b) Detected and recovered AE waveforms due to the point source described in (a).

to I^2R_0, respectively, which were applied to a short section of the thin silver film which was 2 mm wide, 0.5 μm thick, and only 2 mm long between the two brass electrodes. This relatively short length of film acts as a point source of acoustic emission when excited by the current pulse. A dipole time function $D_{xx}(t)$ obtained from Eq. (8) by means of deconvolution of the experimental displacement signal at epicenter, shown in Fig. 6(b) as a solid curve, with the theoretical Green's function shown in Fig. 4(a), is plotted in arbitrary units on the ordinate axis in Fig. 6(a). It should be noted that in all figures having the ordinate axis label "u_z—Displacement," the ordinate actually corresponds to the output of the charge amplifier expressed in units of volts, which is proportional to the normal displacement of the specimen surface $u_z(t)$. Likewise, it is understood that the magnitude of all the source-time functions appearing in the relevant figures is given in terms of arbitrary units. In the work described here, the exact magnitude of these quantities is not required because we are interested only in their temporal behavior. It is noted that the source-time function in Fig. 6(a) is generally a step function with a rise time of about 1.0 μs, which approximately equals that of the input power pulse as shown in Fig. 5(b). This suggests that the temperature rise and hence the thermal dilatation of the film instantaneously follows the input power increment associated with the rising portion of the power curve, whereas the nearly flat portion (with only small variations) of the source-time function after the ramp may be the result of a slow thermal diffusion after the input power begins to decrease abruptly. A similar behavior was observed in the source function associated with Q-pulsed laser heating.[1] The theoretical, synthetic waveform obtained by convolving the dipole source function with the Green's function shown in Fig. 4(a) is displayed as a dotted line in Fig. 6(b). The agreement between the calculated and measured results is seen to be quite good.

It should be pointed out that the contributions to the epicentral displacement for the case of a point source comes not only from D_{xx}, but also from D_{yy}, a horizontal dipole aligned in the y direction, which arises because of the brass electrodes that were attached to the silver film. Since at epicenter both $(D_{xx} * G^P_{xz,x})$ and $(D_{yy} * G^P_{yz,y})$ yield identically the same displacement signals, differing only in magnitude, the overall temporal behavior of the source-time function in Fig. 6(a) is not expected to be affected by the D_{yy} dipole contribution.

Similar procedures were used for analyzing the line source responses for the aluminum thin film. Both excitation current and input power pulses are, respectively, displayed

in Fig. 7(a) and (b), where the maximum applied power to the film is found to be about 15 kW. The Green's functions used for the corresponding analysis are those displayed in Fig. 4(b) for the epicentral response and in Fig. 4(c) for the off-epicentral response. The source function determined from the epicentral response is in Fig. 8(a). It is again observed that the rise time of the source-time function is approximately equal to that of the input power pulse as shown in Fig. 7(b). Synthetic waveforms, generated by the method mentioned previously, compare well to the measured waveforms. The epicentral response is shown in Fig. 8(b) while the off-epicentral response is in Fig. 8(c). Regardless of source type, be it a point or a line source, the short pulse excitation produces essentially the same source-time function, since it is principally determined by the temporal response of the thermal dilatation of the film.

B. Long pulse response

A long-duration, excitation current pulse flowing through a short section of the silver film and the voltage measured across it are shown in Fig. 9(a) and (b), respectively. The pulse duration is seen to be about 17 μs in both figures. The electrical impedance is obtained by dividing the voltage by the current signals and this is displayed in Fig. 9(c) as a solid line whose sharp initial transient may be the result of an inductive reactance. It is seen that after the initial

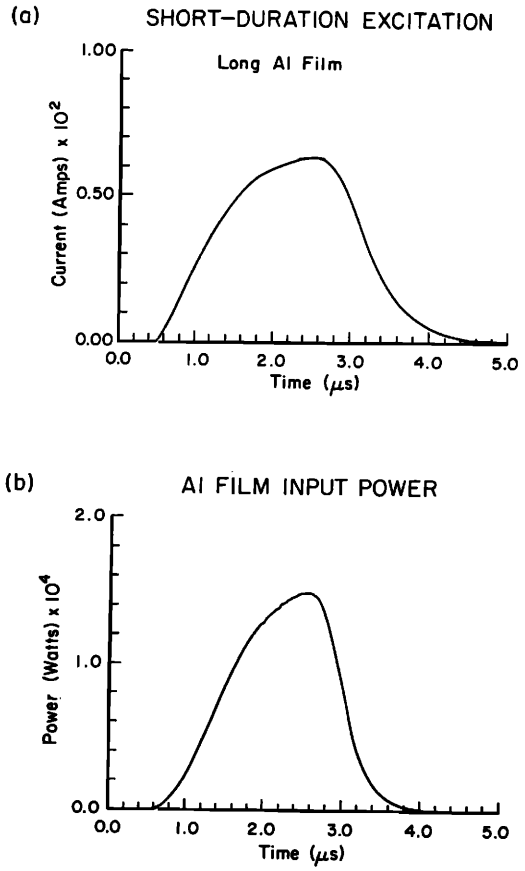

FIG. 7. (a) Short-duration, excitation current pulse applied to a long section of aluminum film. (b) Short-duration, excitation power pulse.

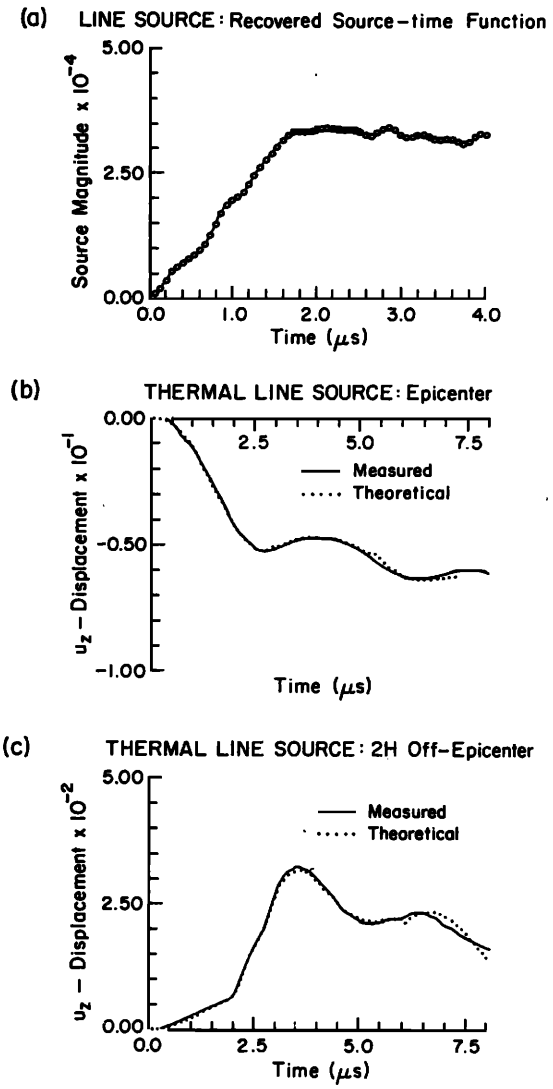

FIG. 8. (a) Line source dipole time function associated with the short-duration current pulse. (b) Detected and recovered waveforms at epicenter due to the line source shown in (a). (c) Detected and recovered waveforms $2H$ away from the epicenter due to the line source shown in (a).

transient, the electrical resistance increases with the film temperature until the current decreases abruptly at the end of the pulse when the transient inductive pick up becomes evident again. Between the two transients at both ends of the pulse lies the contribution of the pure resistance whose temporal behavior was fit with a quadratic polynomial determined by a least-squares method. The polynomial was extrapolated to the time of the arrival of the excitation pulse to permit a determination of the initial electrical resistance R_0 of the film. This is shown as a dotted line in Fig. 9(c). Expressing both R and t in units of (ohms) and (μs), respectively, the result of the curve-fitting yields

$$R(t) = 0.2283 + 0.003\,543\,t - 0.000\,057\,4\,t^2 \quad \text{(ohms)} \tag{12}$$

with a value of the initial resistance, $R_0 = 0.2311\ \Omega$, determined at the arrival of the pulse that occurs at $t = 0.800\ \mu$s. This value of R_0 is in good agreement with that determined

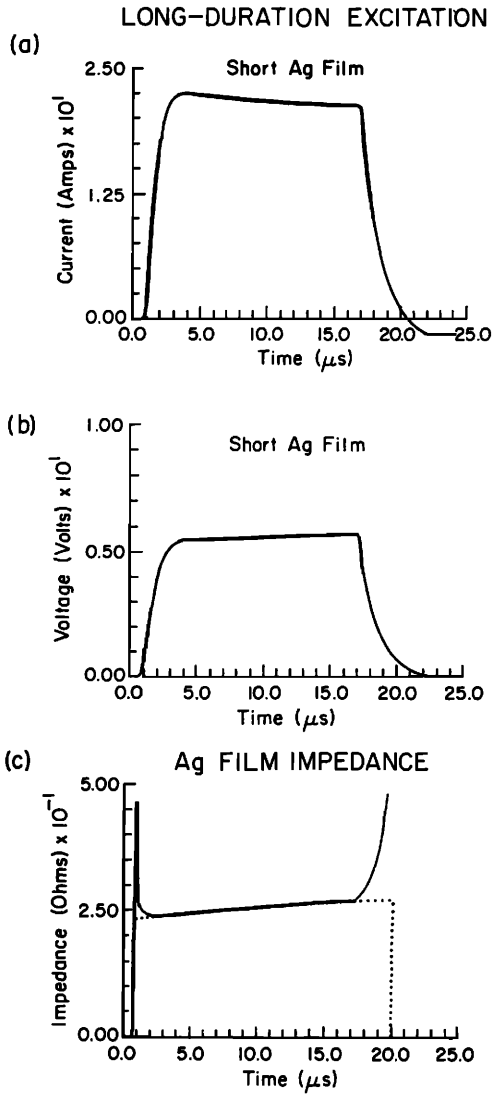

FIG. 9. (a) Long-duration current pulse applied to a short section of the silver film on a glass substrate. (b) Voltage pulse measured across the silver film. (c) Electrical impedance of the silver film as a function of time.

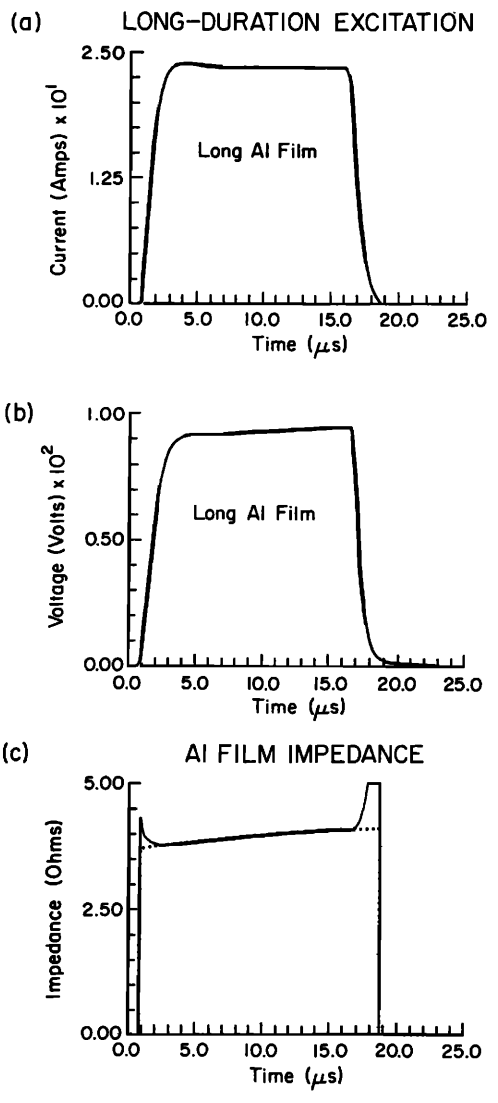

FIG. 10. (a) Long-duration, excitation current pulse applied to a long section of aluminum film on a glass substrate. (b) Voltage pulse measured across the aluminum film. (c) Electrical impedance of the aluminum film as a function of time.

via a static dc measurement.

The same procedure was used to obtain the electrical impedance characteristics of the long aluminum film line source. The excitation current and voltage across the long film are displayed in Fig. 10(a) and (b), respectively. The determined electrical impedance is shown in Fig. 10(c). The result of the curve fit, plotted as a dotted line in Fig. 10(c), is given by analytical expression

$$R(t) = 3.680 + 0.038\,86\,t - 0.000\,860\,5\,t^2 \quad \text{(ohms)}, \tag{13}$$

from which one obtains for the initial resistance at the initial pulse arrival, $R_0 = 3.712\ \Omega$.

The temperature rise θ_f in the aluminum film, which has a temperature coefficient of resistance $\gamma = 4.31\ \text{m}\Omega/\Omega/°\text{K}$, can be obtained from Eq. (3) at any time during the pulse excitation. From the results shown in Fig. 10, the value of θ_f was determined to be 23.7 °C at $t = 17\ \mu\text{s}$ when the excitation pulse abruptly drops to zero.

It is evident from Eqs. (12) and (13) that the temperature increase and hence the thermal dilatation of both the silver and aluminum films is almost linear with time with only a small parabolic term present. The source-time functions of the dipole sources associated with both films are therefore expected to be almost linear functions of time. As Figs. 11(a) and 12(a) show, this was observed both for the silver and for the aluminum films. The results were obtained by deconvolving the measured epicentral displacement signals with their respective Green's functions shown in Fig. 4(a) and (b). A small parabolic contribution is apparently buried in the source-time function because of the numerical noise introduced in the deconvolution process. A comparison between the experimental waveform measured at epicenter and that computed theoretically for a point source in the silver film is shown in Fig. 11(b). Similar comparisons are made for the case of the aluminum film line source both for the epicentral as well as for the off-epicentral responses. The

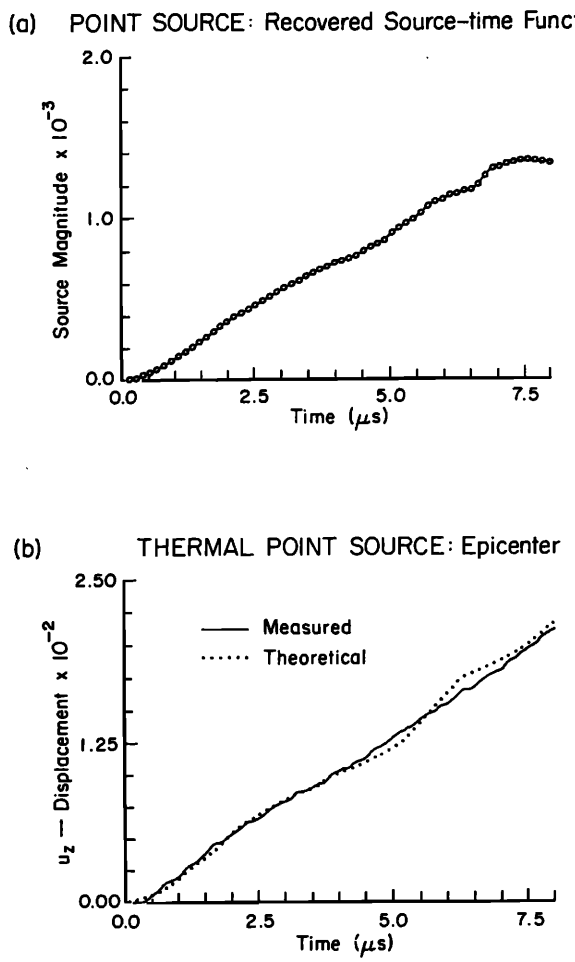

FIG. 11. (a) Point dipole time function associated with the long-duration current pulse. (b) Observed and recovered waveforms due to the point dipole source in (a).

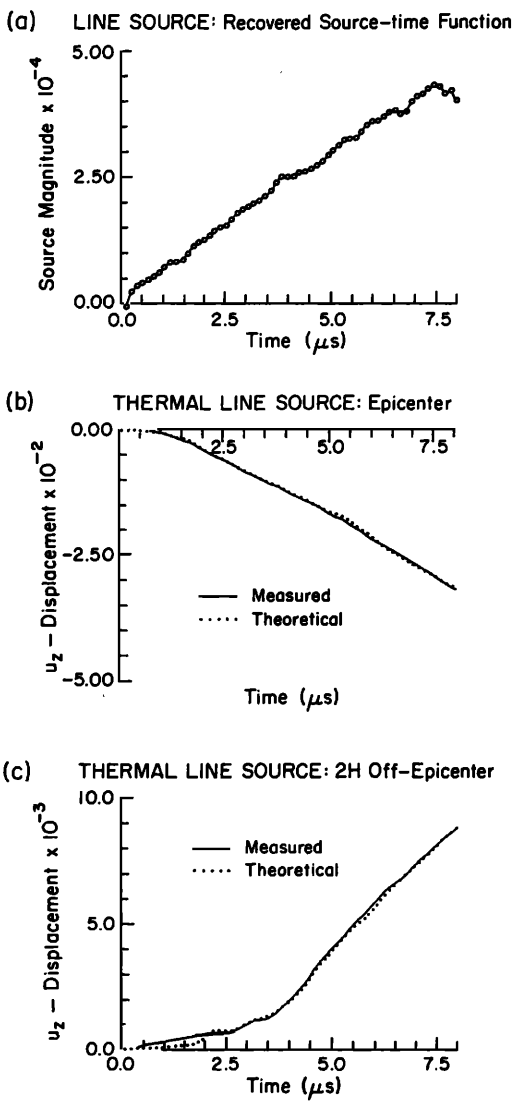

FIG. 12. (a) Line dipole time function associated with the current pulse of long duration. (b) Observed and recovered waveforms at epicenter due to the line source in (a). (c) Observed and recovered waveforms at $2H$ away from the epicenter due to the line source described in (a).

results are shown in Fig. 12(b) and (c). In all cases, the agreement between measured and computed waveforms is found to be excellent.

IV. DISCUSSION

We have presented convincing evidence that elastic waves generated by Joule heating are thermoelastic waves caused by a thermal dilatation source. The thermal strain is a typical example of a more general transformational strain described by Eshelby.[21] The transformational strain is sometimes called a stress-free strain that does not result in a stress, as for instance, inside the heated region of a substrate. It is this transformational strain that characterizes the acoustic emission (AE) source of Joule heating. Other AE sources that can be described by the transformational strain include some phase transformations and plastic deformations. The thermal dilatation source was very well described with a dipole approximation.

A short-duration excitation pulse gave rise to a dipole source-time function that resembled a step function with a short rise time equal to that of the input power pulse. A long-duration excitation pulse resulted in a source-time function that was almost linear in time. If one approximates the source-time function associated with the short-duration excitation pulse by a Heaviside step function, whose integration over time yields a linear ramp function, then the response corresponding to a long-duration excitation pulse will simply be the integration of the short-duration pulse response over time. This fact was confirmed when the displacement curves shown in Figs. 6(b), 8(b), and 8(c) obtained with a short-duration excitation pulse were integrated. The results closely matched the overall shape of the responses obtained with the long-duration excitations shown in Figs. 11(b), 12(b), and 12(c). The integrated curves are not shown in the figures.

The dimensionless constant c in Eq. (7) is left undetermined in this work. However, it can be obtained by performing a simple calibration experiment as described in Ref. 22. Immediately before or after a current excitation pulse is generated, a glass capillary is broken at a point on the top surface of the plate without disturbing the detection system. The

maximum load applied to the glass capillary, measured at the time of fracture, is recorded. The time function of the unloading is essentially a Heaviside step function. Then the value of the dipole strength corresponding to a thermal dilatation of the excitation pulse can be calculated by the procedure detailed in Section 3.4 of Ref. 22. Since all the quantities in Eq. (7), except for c, are known, it can then be easily determined. Conversely, once the constant c and the dipole strength have been determined from an analysis of the emitted signals, the temperature rise of the film can be computed.

Up to now we have discussed the generation of elastic waves from the Joule heating of a thin film. In a similar manner, a small diameter metal wire, which is buried inside an insulator, is expected to also generate a thermoelastic wave when it is suddenly heated. In this case, the source type should be a two-dimensional center of dilatation, lying on a plane perpendicular to the current flow, or a combination of a horizontal and a vertical dipoles, each having equal strength. The time function of such a center of dilatation is also expected to follow the temporal behavior of thermal dilatation, which depends on the mode of excitation as described previously in Sec. II. An example of the waves detected at epicenter is shown in Fig. 13, which was obtained when a short-duration current pulse was used to heat a 0.127-mm-diam platinum wire running midway through an epoxy plate of dimension 7.6 cm long, 7.6 cm wide, and 1.27 cm thick. Because the epoxy plate exhibits a strong viscoelastic behavior for which the plate Green's function is not yet available, a detailed analysis of this signal is not yet possible.

A determination of the thermal properties of the film and the substrate may provide information that is of importance to semiconductor and integrated circuit structures. For investigation of this, it is desirable to have a constant current source whose rise time and associated inductive transients are as short as possible so that an analytical expression can be obtained for the temperature behavior during the pulse excitation, even though the temperature behavior could be obtained with a rigorous numerical method. Such a source would minimize the errors associated with the initial resistance value which, in this work, was obtained by extrapolation. Such an excitation would also result in a source-time function which closely resembles a Heaviside step. Efforts are presently under way to improve the constant current pulse generator so that it can achieve pulse rise times that are less than 0.1 μs.

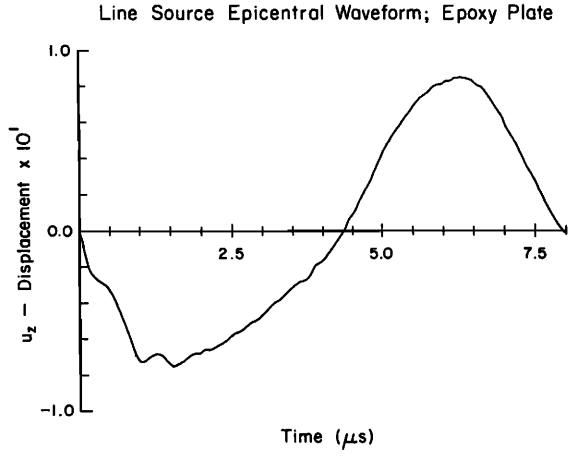

FIG. 13. Observed waveform at epicenter due to a line source located in the middle of an epoxy plate.

V. CONCLUSIONS

Based on the work described here, the following conclusions can be drawn about thermoelastic waves generated by Joule heating sources.

(1) A localized, transient Joule heating generates a thermoelastic wave whose source type is characterized by a dipole or a combination of dipoles.

(2) A short-duration current pulse generates a source whose time function is characterized as a ramp step for which the rise time is approximately equal to that of an input power pulse.

(3) A long-duration current pulse excites a source whose time function corresponds to the temperature increase of the thin film, exhibiting an almost linear behavior in time with a small nonlinear contribution.

(4) The source characterization method described here can be used to study thermal properties of materials and to predict the temperature rise of a heated conductor.

ACKNOWLEDGMENTS

We acknowledge the support of the Office of Naval Research (Physical Acoustics Program) under Contract No. N00014-85-K-0263. Use of the facilities of the Materials Science Center at Cornell, which is funded by the National Science Foundation, is also acknowledged.

[1]C. B. Scruby, R. J. Dewhurst, D. A. Hutchins, and S. B. Palmer, "Laser Generation of Ultrasound in Metals," in *Research Techniques in Nondestructive Testing*, edited by R. S. Sharpe (Academic, London, 1982), Vol. 5, pp. 281–327.

[2]G. Birnbaum and G. S. White, "Laser Techniques in NDE," in *Research Techniques in Nondestructive Testing*, edited by R. S. Sharpe (Academic, London, 1984), Vol. VII, pp. 259–365.

[3]D. A. Hutchins and A. C. Tam, "Pulsed Photoacoustic Materials Characterization," IEEE Trans. Ultrason. Ferroelectric Freq. Control **UFFC-33**, 429–449 (1986).

[4]A. Rosenczwaig, *Photoacoustics and Photoacoustic Spectroscopy*, Vol. 57 in *Chemical Analysis: A Series of Monographs on Analytical Chemistry and its Applications*, edited by P. J. Elving and J. D. Windfordner (Wiley Interscience, New York, 1980).

[5]G. Busse, "Imaging with Optically-generated Thermal Waves," IEEE Trans. Sonics Ultrason. **SU-32**, 355–364 (1985).

[6]A. Rosenczwaig, "Application of Thermal Wave Physics to Microelectronics," in *VLSI Electronic Microstructure Science*, edited by N. Einspruch (Academic, New York, 1985), Vol. 9, pp. 227–287.

[7]G. S. Cargill, "Electron-Acoustic Microscopy," Phys. Today **34**(10), 27–32 (1981).

[8]J. C. Murphy, J. W. Maclachlan, R. B. Givens, F. G. Satkiewicz, and L. C. Aamodt, "The Generation of Ultrasound by Laser, Electron and Ion Probes and its Application to the Characterization of Materials," in *Ultrasonics International '85: Conference Proceedings* (Butterworth Scientific, Surrey, UK, 1985), pp. 30–36.

[9]J. C. Murphy, J. W. Maclachlan, and L. C. Aamodt, "Image Contrast

Processes in Thermal and Thermoacoustic Imaging," IEEE Trans. Ultrason. Ferroelectr. Freq. Control **UFFC-33**, 529–541 (1986).
[10]D. Fournier and A. C. Boccara, "The Mirage Effect in Photothermal Imaging," in *Scanned Image Microscopy*, edited by E. A. Ash (Academic, London, 1980), pp. 347–351.
[11]K. Y. Kim and W. Sachse, "X-ray Generated Ultrasound," Appl. Phys. Lett. **43**, 1099–1101 (1983).
[12]W. Sachse, K. Y. Kim, and W. F. Pierce, "X-ray Generated Ultrasonic Signals: Characteristics and Imaging Applications," IEEE Trans. Ultrason. Ferroelectr. Freq. Control **UFFC-33**, 546–560 (1986).
[13]K. Y. Kim and W. Sachse (unpublished).
[14]K. Y. Kim, L. Niu, B. Castagnede, and W. Sachse, "Miniaturized Capacitive Transducer for the Detection of Broadband Ultrasonic Displacement Signals," Rev. Sci. Instrum. (in press).
[15]H. S. Carlslaw and J. C. Jaeger, *Conduction of Heat in Solids* (Clarendon, Oxford, UK, 1959), 2nd ed., Chap. 12.
[16]G. Jura and W. A. Stark, Jr., "A Technique for Measurement of the Heat Capacity of Metals under Pressure," Rev. Sci. Instrum. **40**, 656–660 (1969).
[17]C. Loriers-Susse and J. P. Bastide, "Specific Heat Measured at High Pressure by a Pulse Method," Rev. Sci. Instrum. **44**, 1344–1349 (1973).
[18]K. Aki and P. G. Richards, *Quantitative Seismology: Theory and Methods* (Freeman, San Francisco, 1980), Vol. I, Chap. 3.
[19]P. M. Morse and H. Feshbach, *Methods of Theoretical Physics* (McGraw-Hill, New York, 1953), Part I, Chap. 7.
[20]A. N. Ceranoglu and Y. H. Pao, "Propagation of Elastic Pulses and Acoustic Emission in a Plate," Trans. ASME, J. Appl. Mech. **48**, 125–147 (1981).
[21]J. D. Eshelby, "The Determination of the Elastic Field of an Ellipsoidal Inclusion and Related Problems," Proc. R. Soc. London Ser. A **241**, 376–396 (1957).
[22]K. Y. Kim and W. Sachse, "Characteristics of an Acoustic Emission Source from a Thermal Crack in Glass," Int. J. Fracture **31**, 211–231 (1986).